32ND INTERNATIONAL COSMIC RAY CONFERENCE, BEIJING 2011

Search for Galactic point-sources of EeV neutrons

BENJAMIN ROUILLÉ D'ORFEUIL[1] FOR THE PIERRE AUGER COLLABORATION[2]
[1]*Kavli Institute for Cosmological Physics and Enrico Fermi Institute, The University of Chicago, Chicago, IL, USA*
[2]*Observatorio Pierre Auger, Av. San Martin Norte 304, (5613) Malargüe, Mendoza, Argentina*
Full author list: http://www.auger.org/archive/authors_2011_05.html
auger_spokespersons@fnal.gov
DOI: 10.7529/ICRC2011/V02/0713

Abstract: The Pierre Auger Observatory has sensitivity to neutron fluxes produced at cosmic ray acceleration sites in the Galaxy. Because of relativistic time dilation, the neutron mean decay length is $(9.2 \times E)$ kpc, where E is the neutron energy in EeV. A blind search over the field of view of the Auger Observatory for a point-like excess yields no statistically significant candidates. The neutron flux upper limit is reported as a celestial function for three different energy thresholds. Also a search for excesses of cosmic rays in the direction of selected populations of candidate Galactic sources is performed. The bounds obtained constrain models for persistent discrete sources of EeV cosmic rays in the Galaxy.

Keywords: Pierre Auger Observatory; high-energy neutron sources; neutron flux limits.

1 Motivations for EeV neutron astronomy

At EeV (1 EeV = 10^{18} eV) energies, the Galactic magnetic field isotropizes the charged particle fluxes, making it impossible to pick out possible Galactic proton sources. On the other hand, neutron astronomy inside our Galaxy is possible. Neutrons travel indeed undeflected by magnetic fields, and their mean decay length $\lambda_{\rm n} = (9.2 \times E)$ kpc, where E is the neutron energy in EeV, is comparable to the Earth distance from the Galactic center. Hence, neutron induced extensive air showers (EAS) could produce a directional excess of cosmic rays (CRs) in the sky, clustered within the observatory's angular resolution.

High energy neutrons can be produced by the interaction of accelerated protons or heavier nuclei with the radiation and baryonic backgrounds inside the sources or in their surroundings. They can take over most of the initial CR energy per nucleon and would not be magnetically bound to the accelerating region. Gamma-rays can also be generated via these interactions, but they acquire a lesser fraction of the primary CR energy.

If one assumes that CRs are produced with a continuous power-law spectrum that extends from GeV to EeV with an injection spectral index of -2, the energy deposited in each decade should be comparable. Accordingly, the observed GeV-TeV gamma-ray fluxes, provided that they have a significant component of hadronic origin, would motivate the search for neutron fluxes in the EeV range.

In terms of high energy CR astrophysics, it is crucial to look for Galactic sources that could accelerate particles up to EeV energies. A time-honored picture is that the transition between particles produced in Galactic and extragalactic sources happens at the 'ankle', a hardening of the slope in the CR energy spectrum appearing in the middle of the EeV energy decade [1], that could naturally be explained by the emergence of a dominant extragalactic component (see [2] for a review). This model requires that particles be accelerated above ~ 1 EeV by sources inside our Galaxy.

2 Methodology

The array of surface detectors (SD) of the Pierre Auger Observatory is used to search for point-like excesses at EeV energies that would be indicative of a flux of neutral particles from a discrete source. The sensitivity of the SD in this energy range and its large aperture ensures that constraining limits can be set over a large fraction of the sky. These upper limits will be interpreted as upper limits on neutron fluxes since (i) above any fixed energy, the emission rate of neutrons from a CR source in our Galaxy is expected to be well above the emission rate of gamma-rays of hadronic origin and (ii) in the search for an excess of arrival directions in a small solid angle, the SD is far more sensitive to neutrons than to gamma-rays. Indeed, roughly half of the signal in hadronic EAS is due to muons traversing the water Cherenkov-stations. Gamma-ray EAS, being muon poor, should, for a given energy, produce a smaller signal, they hence have a reduced trigger efficiency and are also harder to identify in the larger background of lower energy CRs.

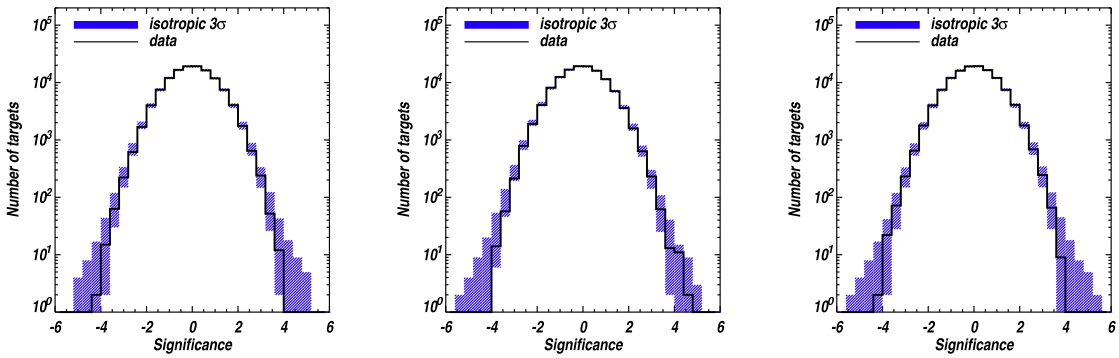

Figure 1: Distribution of the Li-Ma significances of the blind searches together with the 3σ containment of 5000 Monte-Carlo samples of an isotropic sky. From left to right: $[1-2]$ EeV, $[2-3]$ EeV, and $E \geq 1$ EeV.

We perform here two analyses to constrain the neutron flux from Galactic sources in three energy bands: $[1-2]$ EeV, $[2-3]$ EeV, and $E \geq 1$ EeV. First, a blind search for localized excesses in the CR flux over the exposed sky was carried out. The search compared the number of observed events with that expected from an isotropic background, in top-hat counting regions matching the angular resolution of the instrument. Flux upper limits were derived and plotted on celestial maps. Second, a stacking analysis was performed in the direction of bright Galactic gamma-ray sources detected by the Fermi LAT (100 MeV – 100 GeV) and the H.E.S.S. (100 GeV – 100 TeV) telescopes.

These analyses use high quality events with zenith angles $\theta < 60^\circ$ recorded by the SD between 1 January 2004 and 30 October 2010. Periods of unstable acquisition were removed. More than 340000 SD events have been reconstructed with energies above 1 EeV.

3 Blind search over the covered sky

To study the possible presence of overdensities, one needs first to obtain the background expectations for the different sky directions under the assumption of an isotropic CR distribution. This is achieved by parametrizing the zenith angle distribution of the observed events in the energy range under study to smooth out statistical fluctuations [3].

Sensitivity to point sources is optimized by matching the target region size to the angular resolution of the instrument. The angular resolution of the SD, ψ, corresponding to the 68% containment radius, is better than 1.8° and 1.5° above 1 EeV and 2 EeV, respectively [5]. For a gaussian point spread function characterized by σ, the signal-to-noise ratio is optimized for a top-hat radius given by $1.59\sigma = 1.05\psi$.

We use an HEALPix [4] grid with resolution parameter $N_{\rm side} = 128$ to define the center point of each target region. The size of a pixel being small ($27.5'$) compared to a target region, there is a significant overlap between neighboring targets. The number of arrival directions (observed or expected) in any target is taken as the sum of the counts in the pixels (using a higher resolution: $N_{\rm side} = 1024$) whose center is contained in the target region.

We evaluate the Li-Ma significance[1] [6] in each target. The distribution of the significances of the blind searches are shown in Figure 1. The blind search over the field of view (FOV) of the SD reveals no candidate point on the sky that clearly stands up above the expected distribution of significances in isotropic simulations (shaded region). It is therefore sensible to derive a flux upper limit in each target.

We adopt the definition of [7] to compute the upper limit $\bar{s}_{\rm UL}$ of confidence level $\mathrm{CL} = 1-\alpha$ on the expected signal $\bar{s}$, when an observation results in a count n in the presence of a Poisson background distribution with mean value $\bar{b}$:

$$P(\leq n|\bar{b}+\bar{s}_{\rm UL}) = \alpha \times P(\leq n|\bar{b}) \qquad (1)$$

The CL is set to 95%. For each target we derive the bounds on the neutron flux by dividing $\bar{s}_{\rm UL}$ by the exposure (in km^2 yr). The latter is obtained by dividing, for each region, the expected number of background events per target solid angle by the intensity of CRs in the energy bin under study, which is obtained from the measured CR energy spectrum [1]. As the target circle encompasses 71.75% of the total gaussian-distributed signal, the final upper limit to the flux is obtained by scaling the above bound by 1/0.7175. Figure 2 presents sky maps of the flux upper limits for the three energy bins considered for the analysis. The upper limits become less stringent near the border of the FOV because of the reduced statistics. We hence only present the results for $\delta < 15^\circ$ to avoid the lowest exposure regions.

Note that if the background were due to a heavier composition, since the efficiency for detection of heavy nuclei is expected to be slightly larger at EeV energies than for the potential neutron signal, the bounds could be slightly relaxed. We note however that the measurements of the depth of shower maximum are consistent with a predominantly light composition at EeV energies [8].

The galactic center is a particularly interesting target because of the presence of a massive black hole. The results

1. For the α parameter in the expression of the Li-Ma significance, we use $\alpha_{\rm LM} = n_{\rm exp}/n_{\rm tot}$ with $n_{\rm exp}$ the background expected in the target and $n_{\rm tot}$ the total number of events.

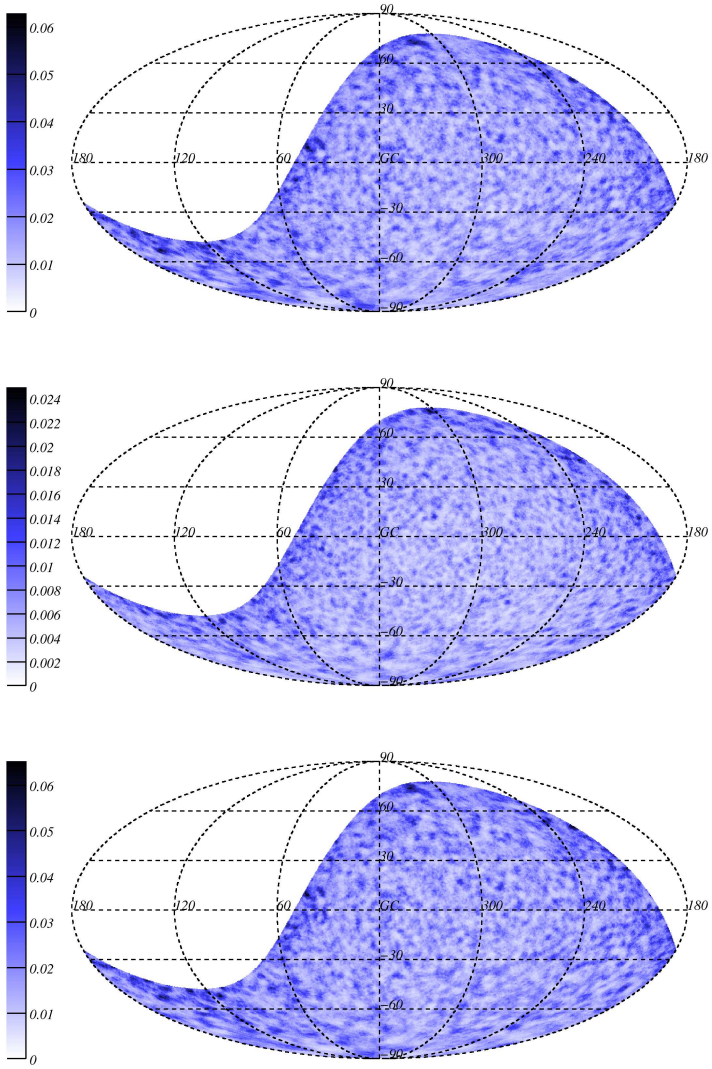

Figure 2: Flux upper limits celestial maps (in unit of km^{-2} yr^{-1}) in Galactic coordinates. From top to bottom: $[1-2]$ EeV, $[2-3]$ EeV, and $E \geq 1$ EeV.

for the window centered on it and for $E \geq 1$ EeV shows no excess ($S = -1.43$) and hence we obtain a 95% CL upper limit on the flux from a point source in this direction of 0.01 km^{-2} yr^{-1}, which updates the bounds obtained previously in [9]. We note that for directions along the Galactic plane the upper limits are below 0.024 km^{-2} yr^{-1}, 0.014 km^{-2} yr^{-1} and 0.026 km^{-2} yr^{-1} for the energy bins $[1-2]$ EeV, $[2-3]$ EeV and $E \geq 1$ EeV, respectively.

4 Targeted search

The targeted search involves the selection of bright gamma-ray sources and the search for an excess in their directions. We define the excess signal in a solid angle Ω around one source as: $S = N_{\rm s}/\sqrt{N_{\rm iso}}$, where $N_{\rm s}$ is the difference between the observed and expected ($N_{\rm iso}$) number of events in the target region around each source.

In order to improve the signal over background, we perform a stacking analysis on sets of $\mathcal{N}_{\rm s}$ sources. The stacked excess signal reads $S_{\rm stacked} = \sum N_{\rm s}/\sqrt{\sum N_{\rm iso}}$ and scales as $S\sqrt{\mathcal{N}_{\rm s}}$ for the ideal case in which sources producing equal neutron flux on Earth are detected with uniform coverage.

The acceleration of particles above 1 EeV by sources inside our Galaxy is theoretically challenging. The most powerful Galactic objects either do not possess the required luminosity to accelerate particles to such high energy, or present acceleration environments that are too dense for particles to escape without losing energy. Pulsars and Pulsar Wind Nebulæ (PWN) however are considered to be good potential accelerators (see e.g., [10, 11]), and recent work shows

that the maximum energy of accelerated iron nuclei may reach 5 EeV in certain supernova remnants (SNR) [12]. Models predicting the production of neutrons at EeV energies from powerful Galactic sources have also been discussed (e.g., [13, 14]). The candidate sources are expected to be strong gamma-ray emitters at GeV and TeV energies.

For this reason, we apply this analysis to Galactic gamma-ray sources extracted from the Fermi LAT Point Source Catalog [15] and the H.E.S.S. Source Catalog[2], focussing on pulsars, PWN and SNR. Targets were selected among the sources located in the portion of the Galactic plane, defined as $|b| < 10^\circ$, covered by the FOV of the SD, and located at a distance shorter than 9 kpc ($\lambda_{\rm n}$ at 1 EeV). As an example, we built two sets by selecting from each catalog the ten brightest sources (in flux observed on Earth) fulfilling these criteria. Our targets are listed in Tables 1 and 2.

Name 1FGL	l [deg]	b [deg]	distance [kpc]
J0835.3-4510	263.55	-2.79	0.29 ± 0.02
J1709.7-4429	343.10	-2.69	$1.4 - 3.6$
J1856.1+0122	34.70	-0.42	2.8
J1809.8-2332	7.39	-1.99	1.7 ± 1.0
J1801.3-2322c	6.57	-0.21	1.9
J1420.1-6048	313.54	0.23	5.6 ± 1.7
J1018.6-5856	284.32	-1.70	2.2
J1028.4-5819	285.06	-0.49	2.3 ± 0.7
J1057.9-5226	285.98	6.65	0.7 ± 0.2
J1418.7-6057	313.33	0.14	$2 - 5$

Table 1: Set of bright sources selected from the Fermi LAT Point Source Catalog. Distances are from [16] and the references cited in [17].

Name HESS	l [deg]	b [deg]	distance [kpc]
J0852-463	266.28	-1.24	0.2
J0835-455	263.85	-3.09	0.29
J1713-397	347.28	-0.38	1
J1616-508	332.39	-0.14	6.5
J1825-137	17.82	-0.74	3.9
J1708-443	343.04	-2.38	2.3
J1514-591	320.33	-1.19	5.2
J1809-193	10.92	0.08	3.7
J1442-624	315.41	-2.30	2.5
J1640-465	338.32	-0.02	8.6

Table 2: Set of bright sources selected from the H.E.S.S. Source Catalog. Distances are from the TeVCat catalog (http://tevcat.uchicago.edu/).

The stacked signal computed from the SD data at the positions of the two sets of sources are presented in Table 3 for the three energy bins under study. No excess is found.

Set of sources	Energy bin [EeV]	$S_{\rm stacked}$
Table 1	$[1-2]$	2.07
Table 1	$[2-3]$	0.51
Table 1	≥ 1	2.35
Table 2	$[1-2]$	-0.75
Table 2	$[2-3]$	-0.40
Table 2	≥ 1	-0.89

Table 3: Application to sets of sources (Tables 1 and 2). Stacked excess signals, $S_{\rm stacked}$ derived for the SD data.

5 Conclusion

The data recorded by the Auger Observatory in the EeV energy range has been used to search for point like excesses that would be indicative of a flux of neutrons from Galactic sources. Two analyses were performed, (i) a blind search of the exposed sky and (ii) a stacking analysis in the direction of bright gamma-ray sources detected by the Fermi LAT and H.E.S.S. telescopes. Both analyses reveal no statistically significant excess. Upper limits were calculated for all parts of the sky. Above 1 EeV, the flux upper limit is less than 0.065 km^{-2} yr^{-1} corresponding to an energy flux of 0.13 EeV km^{-2} yr^{-1} $\simeq 0.4$ eV cm^{-2} s^{-1} in the EeV decade assuming an $1/E^2$ differential energy spectrum.

References

[1] The Pierre Auger Collaboration, Phys. Lett., 2010, **B685**: 239-246
[2] K. Kotera, A. V. Olinto, ARAA, 2011, **49**: 119-53
[3] J.-Ch. Hamilton, for the Pierre Auger Collaboration, Proc. 29th ICRC, Pune, India, 2005, **7**: 63-66
[4] K. M. Górski *et al.*, ApJ, 2005, **622**: 759-771
[5] C. Bonifazi, for the Pierre Auger Collaboration, Nucl. Phys. B (Proc. Suppl.), 2009, **190**: 20-25
[6] T.-P. Li, Y.-Q. Ma, ApJ, 1983, **272**: 317-324
[7] G. Zech, Nucl. Instrum. Meth., 1989, **A277**: 608-610
[8] The Pierre Auger Collaboration, PRL, 2010, **104**: 091101
[9] The Pierre Auger Collaboration, Astropart. Phys., 2007, **27**: 244-253
[10] M. Giller, M. Lipski, J. Phys., 2002, **G28**: 1275-1286
[11] W. Bednarek, M. Bartosik, A&A, 2004, **423**: 405-413
[12] V. Ptuskin, V. Zirakashvili, E.-S. Seo, ApJ, 2010, **718**: 31-36
[13] D. Grasso, L. Maccione, Astropart. Phys., 2005, **24**: 273-288
[14] F. Aharonian, A. Neronov, ApSS, 2005, **300**: 255-265
[15] A. A. Abdo *et al.*, ApJS, 2010, **188**: 405-436
[16] D. A. Green, Bull. Astron. Soc. India, 2009, **37**: 45-61
[17] A. A. Abdo *et al.*, ApJS, 2010, **187**: 460-494

2. http://www.mpi-hd.mpg.de/hfm/HESS/pages/home/sources/